Distinguishing Single- and Double-Stranded Nucleic Acid Molecules Using Solid-State Nanopores

ARTICLE *in* NANO LETTERS · JULY 2009

Impact Factor: 13.59 · DOI: 10.1021/nl901370w · Source: PubMed

5 AUTHORS, INCLUDING:

Gary Mark Skinner
Illumina
20 PUBLICATIONS **387** CITATIONS
SEE PROFILE

Michiel van den Hout
FOM Foundation for Fundamental Researc…
14 PUBLICATIONS **383** CITATIONS
SEE PROFILE

Nynke Dekker
Delft University of Technology
144 PUBLICATIONS **4,162** CITATIONS
SEE PROFILE

NANO LETTERS

2009
Vol. 9, No. 8
2953-2960

Distinguishing Single- and Double-Stranded Nucleic Acid Molecules Using Solid-State Nanopores

Gary M. Skinner,† Michiel van den Hout,† Onno Broekmans, Cees Dekker, and Nynke H. Dekker*

Kavli Institute of Nanoscience, Delft University of Technology, Lorentzweg 1, 2628 CJ Delft, The Netherlands

Received April 29, 2009; Revised Manuscript Received June 11, 2009

ABSTRACT

Solid-state nanopores offer a promising method for rapidly probing the structural properties of biopolymers such as DNA and RNA. We have for the first time translocated RNA molecules through solid-state nanopores, comparing the signatures of translocating double-stranded RNA molecules and of single-stranded homopolymers poly(A), poly(U), poly(C). On the basis of their differential blockade currents, we can rapidly discriminate between both single- and double-stranded nucleic-acid molecules, as well as separate purine-based homopolymers from pyrimidine-based homopolymers. Molecule identification is facilitated through the application of high voltages (~600 mV), which contribute to the entropic stretching of these highly flexible molecules. This striking sensitivity to relatively small differences in the underlying polymer structure greatly improves the prospects for using nanopore-based devices for DNA or RNA mapping.

Because of their central importance within the machinery of life, nucleic acid structures, such as the DNA double-helix, RNA hairpins, RNA pseudoknots, and so forth, have been intensively studied. Given their nanometer-scale sensitivity and ability to probe dynamics in real time, single-molecule techniques have recently provided a new tool for the investigation of these elastic molecules.[1,2] For example, force spectroscopy techniques such as optical tweezers have been used to study the unfolding of single RNA structural motifs.[3,4] A novel single-molecule tool that allows for the detection of local molecular structure has emerged in the form of nanopores.[5–7] As molecules translocate through a nanopore carrying an ionic current, a portion of the current is blocked, resulting in a characteristic blockade of the pore that depends upon the molecule that is translocating.[8,9] In principle, these pores could be used to rapidly identify and map local structures along biopolymers.

Naturally occurring nanopores have been employed in many translocation studies, for example, the α-Hemolysin (α-HL) protein,[10] which forms a continuous channel across a lipid bilayer.[11] These α-HL nanopores have been used to probe DNA translocations,[8,12,13] including forced unzipping of the double-helix.[14] They have also been used to discriminate the differing structural nature of RNA homopolymers.[15] However, this discrimination relies on the unique translocation dynamics of each molecule and strongly depends upon the interaction of the RNA molecules directly with the pore surfaces. In addition, the use of a protein-based pore limits the kinds of analysis to only systems at close to physiological conditions of temperature, pH, denaturants, etc. Furthermore, the small size of the α-HL pore (diameter ~1.3 nm),[10] also limits biomolecular analysis to molecules of this order of size, for example, dsDNA cannot pass through α-HL.[8]

For these reasons, efforts have been directed toward the development of artificial nanopores fabricated using existing semiconductor technologies.[16,17] Such solid-state nanopores have been used to measure local force upon DNA arrested within a pore,[18–20] nucleic-acid unzipping,[21] and protein/DNA complexes.[9] Here, we have translocated single-stranded (ss) RNA homopolymers poly(A),[22] poly(C),[23] poly(U),[24] and double-stranded (ds) A-RNA. We have measured the pore conductance that is blocked by these molecules while sweeping the applied bias from 100 to 600 mV. This conductance blockage versus applied bias relationship is distinctly nonlinear for both classes of molecules with the double-stranded molecules blocking more conductance as a function of voltage, while the single-stranded molecules block less. This differing response to voltage allows one to readily identify molecule type.

Methods. ***Nanopores.*** We employed solid-state nanopores for the investigation of single- and double-stranded nucleic acid polymers. Nanopores of approximately 10 nm in diameter were drilled into freestanding 20 nm thick Silicon Nitride membranes, using a 300 keV transmission electron

* To whom correspondence should be addressed. E-mail: N.H.Dekker@tudelft.nl. Tel: +31-(0)15-27 83219. Fax: +31-(0)15-27 81202.
† These authors contributed equally to this work.

10.1021/nl901370w CCC: $40.75
Published on Web 06/19/2009

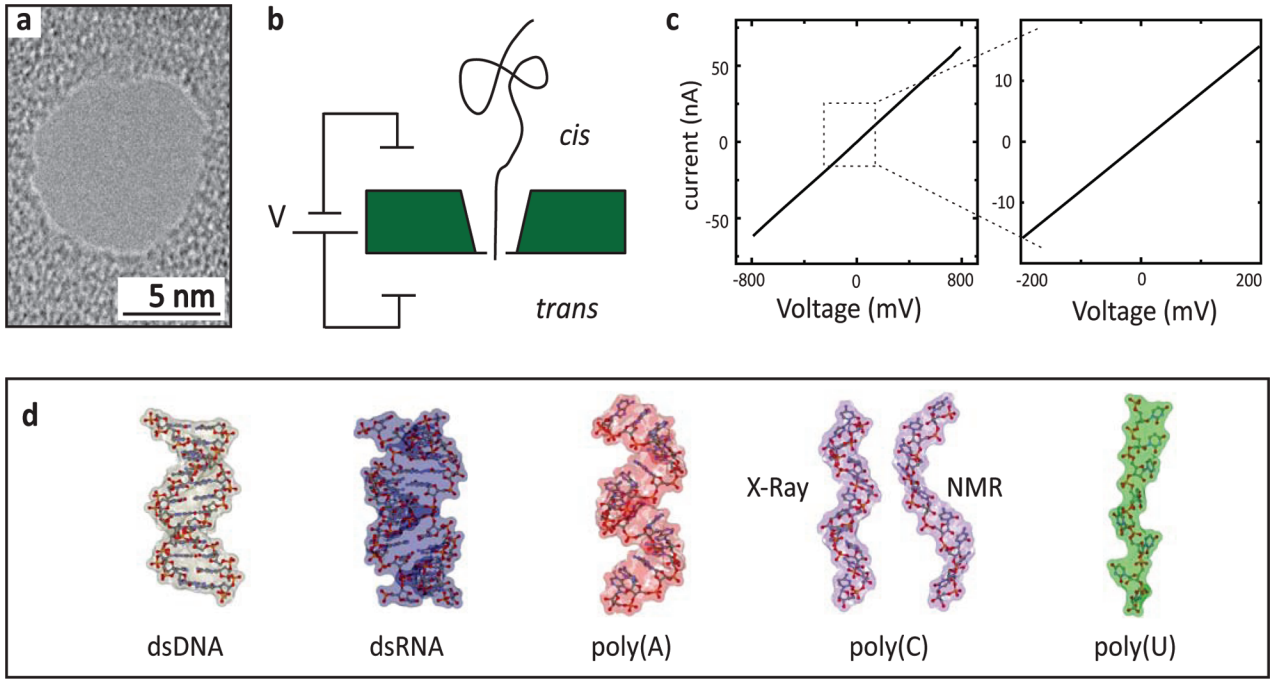

Figure 1. Experimental setup and molecules used for translocation experiments. (a) A representative transmission electron micrograph of the nanopores used in these experiments. (b) Schematic of the experiment; green represents the nanopore-containing chip. A pair of electrodes is inserted into each reservoir for bias application and current measurement. (c) Typical $I-V$ curves for one of our solid-state nanopores. The righthand panel is a zoom in on the low voltage regime of ±200 mV. (d) Atomic models of each of the nucleic-acid polymers used in this study with surface enclosing molecular volume applied. In the case of poly(C) there are two proposed structural models, a right-handed helix determined by X-ray studies[23] and a left-handed helix, suggested from NMR studies.[29]

microscope.[17] Figure 1a shows an example TEM image of one of our pores. Prior to drilling, the surface of the chip containing the pore was coated in a layer of PDMS, extending to within a few tens of micrometers from the edge of the free-standing SiN membrane.[43] Immediately after electron-beam drilling, the pore was submerged within a solution of 20 nm filtered 50:50 ethanol/dH2O until use. We found that these two simple steps yielded a far greater number of useable pores and also significantly improved the signal-to-noise ratio of our pores. Our solid-state nanopores exhibit good low-noise (∼5−15 pA I_{rms} at 100 mV at 1 kHz low-pass filter).

The nanopore-containing chip was mounted within a custom-built Teflon flowcell containing two reservoirs for the introduction of ionic solutions containing the various molecules under study. A schematic of the setup is shown in Figure 1b. The flowcell has ports that allow for the independent introduction of the various desired solutions into either chamber of the flowcell. Additional ports allow for the connection of the nanopore device to an Axon Instruments Axopatch 200B amplifier. Pore resistance was determined by measuring the pore current as a function of applied bias voltage and applying a linear fit to the slope of the resulting IV plot (Figure 1c). Nucleic-acid molecules for study (Figure 1d; see also below) were introduced in 10 mM Tris-HCl (pH 8.0), 1 mM EDTA, 1 M KCl, onto one side of the nanopore chip, and a voltage bias was applied across the silicon nitride membrane. The voltage and current were sampled at 150 kHz or higher bandwidth, and subsequently low-pass filtered at 35 up to 70 kHz. For each molecule, traces of translocation events were collected at many different applied bias voltages, ranging from 100 mV up to 600 mV. After low-pass filtering the traces translocation events were identified based on preset selection criteria as described earlier[25] (see Supporting Information, Figure S1).

For each data set, the filter frequency was chosen such that peak amplitudes in the current were not significantly affected by the filter. This was done by comparing the extreme values of the filtered detected events with the unfiltered raw data (see Supporting Information, Figure S2). The current traces of each event together with a small number of baseline (i.e., open pore current) points around it were each normalized by subtracting the average baseline value and then added together into a single long trace. Examples of such traces and histograms of these traces are shown in Figure 2. To ensure that most of the detected events correspond to actual translocations, a simple check is performed; prior to each measurement, we ensure that no events are observed upon applying a negative bias voltage, that is, no molecules translocate from trans to cis. Then, right after an actual measurement where translocations from cis to trans have been observed, the same check is performed; a small number of translocations are observed, which then cease after several seconds. This is a clear indication that molecules actually traversed the pore, and molecules that recently translocated can be recaptured into the pore.[26] However, such events quickly cease as the majority of the translocated molecules will have diffused away from the pore.

Synthesis of Molecules. Single-stranded homopolymers of poly(A), poly(C), and poly(U) were synthesized by

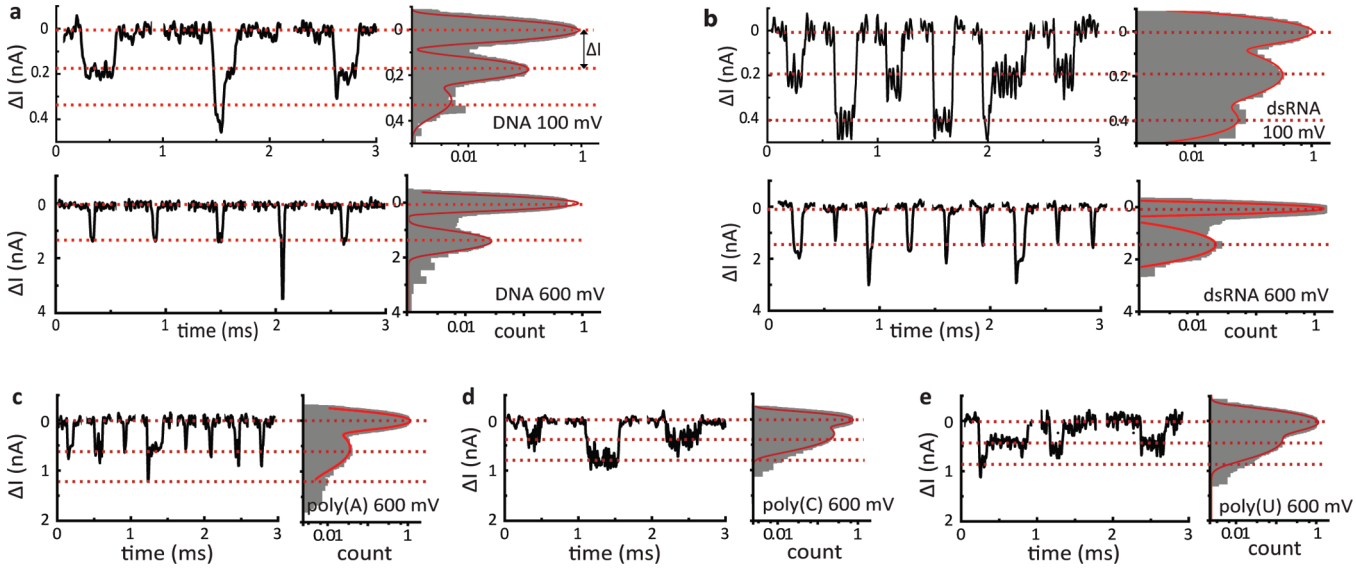

Figure 2. Examples of translocation events. Here we show sample events as well as complete histograms for all molecules studied. (a) dsDNA; (b) dsRNA; (c) poly(A); (d) poly(C); and (e) poly(U). DsDNA and dsRNA are shown at both low (100 mV) and high (600 mV) bias. All other molecules are shown at 600 mV. In each case, the lefthand panel shows sample events, while the righthand panel shows a typical histogram of the nanopore current, normalized to the baseline current when the pore is empty. The peak current blockade for each molecule at a given voltage was determined from the mean of the Gaussian fitted to the first peak. The resulting ΔI levels at a given voltage are indicated by red dashed lines.

incubating 20 mM of ADP, CDP, and UDP, respectively, with polynucleotide phosphorylase (PnP) (Sigma Aldrich) at 37 °C for 20 min in a buffer containing 100 mM Tris-HCl pH 9.0, 5 mM MgCl2, 0.4 mM EDTA, and 4% BSA. For dsRNA, a random-sequence polydisperse length heteropolymer was synthesized using PnP and equimolar rNDPs. This ssRNA molecule was then converted to dsRNA by use of the RNA dependent RNA polymerase from phage Φ6.[27] From gel electrophoresis, we estimated the length distributions to be 10 to 20 kb for poly(A) and poly(U), 3−10 kb for poly(C), and 10−30 kb for the ds A-RNA molecules. We used a 12.7 kb ds B-DNA fragment produced by PCR amplification from a 2λ-phage DNA template (Promega).[28]

Molecular Modeling and Volume Computation. Molecular models of the known structures of each of the molecules are shown in Figure 1d. ds B-DNA and ds A-RNA are double-stranded and have a helical diameter of ∼2.0 and ∼2.3 nm respectively (as we deduced from the crystal structures (pdb ID no. 2BNA and 3CIY (minus protein), respectively). For the single-stranded RNA molecules, poly(A) is known to form a helical structure with a diameter of 2.1 nm.[22] In the case of poly(C), there are two alternative models for the structure, a right-handed helix of 1.3 nm diameter as determined from X-ray studies[23] or a left-handed 1.7 nm diameter helix determined through the use of H1 NMR[29] (both shown in Figure 1d). Poly(U) instead adopts a random coil in solution with an effective diameter of ∼1.3 nm as determined from our molecular modeling (Figure 1d). For the fully stretched homopolymers, all-atom models of 15−20 bases of each fully stretched linear molecule ($x/L_0 \sim 1$) were constructed using Xenoview software.[30] These structures correspond to how these polymers would appear when extended under very high forces (∼50 pN). The helical homopolymer structures were built using Accelrys DS Visualizer (Accelrys, Inc.) taking the structural data previously reported for poly(A)[22] and the two poly(C) structures mentioned above.[23,29] For the ds B-DNA, we used pdb ID no. 2BNA[31] and 3CIY[32] for the dsRNA, after deletion of the bound protein, which does not distort the ds A-RNA helix. Each model was imported into the software package VEGA ZZ (Università degli Studi di Milano) to calculate its molecular volume; we define this to be the solvent inaccessible volume using a probe radius of 2.0 Å. The resulting pdb files for each of the homopolymers are available upon request.

Results. Examples of translocation events for each of the molecules at different applied bias values are shown in Figure 2a−e, left panels. Each event is characterized by the amplitude of the current blockade, ΔI, and by the length of time the molecule spends in the pore. ΔI is defined as the open pore current (I_{open}) minus the current in the blocked state ($I_{blocked}$), resulting in positive values for all experiments presented here. Events were identified (see Nanopores, above, as well as Supporting Information) and used to construct histograms of the current values during the blockade events (Figure 2a−e, right panels).

In this study, ds B-DNA was used as a calibration tool (Figure 2a) to which the properties of the other molecules under study are compared. The mean current blockade, ΔI, was determined from a Gaussian function fitted to the first peak in the current histogram (in all cases, the peak number is relative to that of the open pore current). At low voltage, we measure a ΔI corresponding to a mean conductance change, ΔG (= $\Delta I/V$) of 1.6 ± 0.5 nS at 100 mV, consistent with previous measurements of the same parameter for ds B-DNA.[33−36] Additional peaks in the current histogram are also observed at integer multiples of this ΔI. As shown in previous work, the first peak corresponds to DNA passing

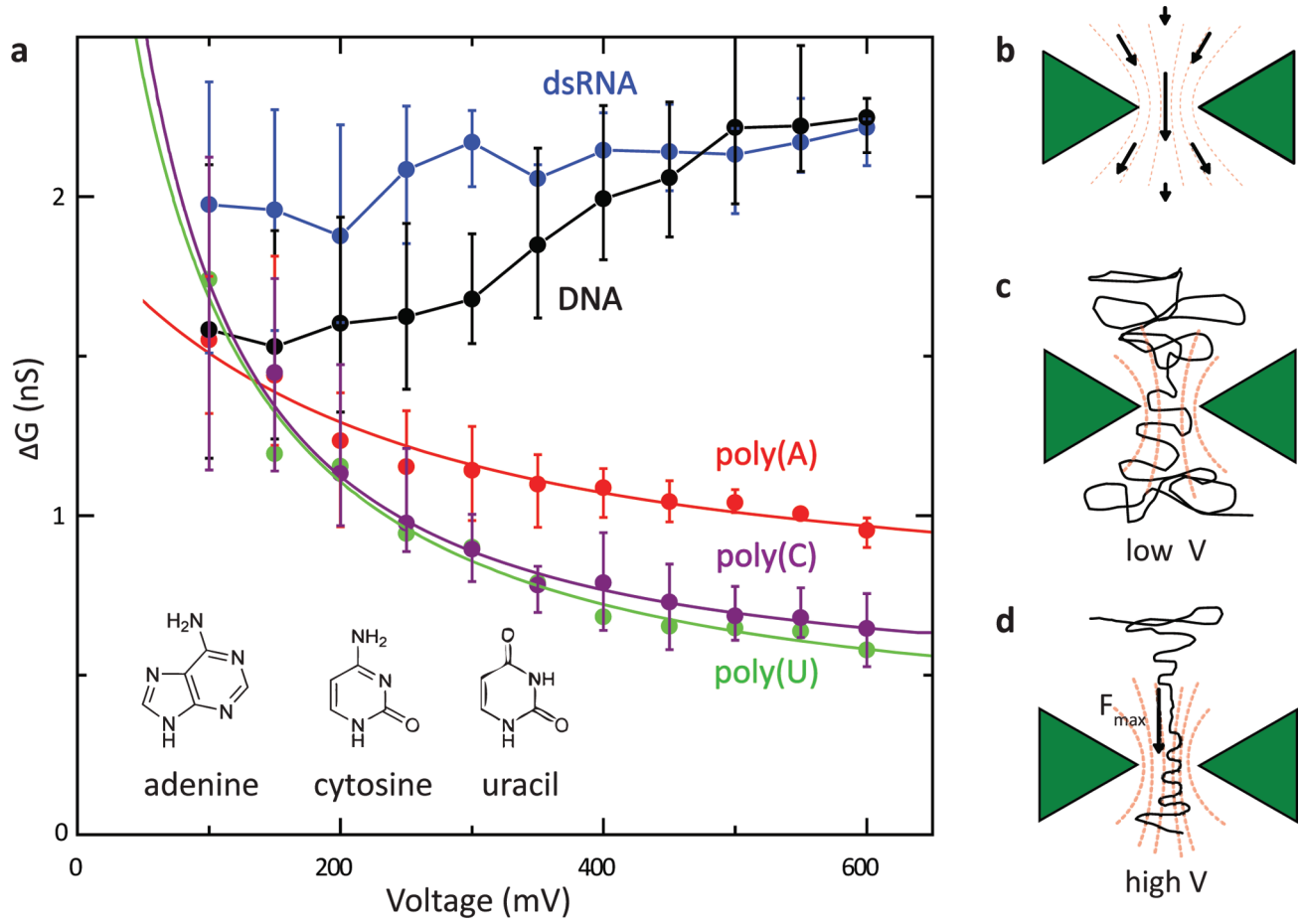

Figure 3. Relationship between the applied bias and the amplitude of the conductance blockade. (a) Plot of the change in pore conductance, ΔG, as a function of applied bias across the nanopore ($\Delta G = (I_{open} - I_{blocked})/V$). At each voltage, a single experiment with a given nanopore contributed many hundreds of events, for which ΔI, and hence ΔG, were determined by fitting (see Figure 2). Points shown on this plot are the mean values from N independent experiments at a given voltage, where $N = 2$ for dsRNA (blue), $N = 3$ for dsDNA (black), $N = 7$ for poly(A) (red), $N = 2$ for poly(C) (violet), and $N = 1$ for poly (U) (green). Errors bars represent the maximum and minimum values from the N experiments. For poly (U), the error bars are left out as only one measurement was performed ($N = 1$). The solid red, green, and violet lines are fits to a model assuming the polymers are entropically stretched inside the pore (see main text). A version of this figure with all separate measurement points is available in the Supporting Information (Figure S6). (b) The force exerted upon a charged particle that experiences the electric field within the pore is proportional to the field strength at that location. Black arrows represent the magnitude of this force. (c) At low V, these stretching forces are lower, and the highly flexible ($L_p \sim 1$ nm[38,39]) homopolymers have low relative extension, thus occupying more of the pore volume. (d) At high V, the stretching force is higher, and so the molecule has a higher relative extension, occupying less of the pore volume, resulting in a lower measured ΔG. The stretching force is a combination of the electrical force and drag forces on the polymer, and varies along the nanopore, reaching a peak somewhere above the pore.

through the pore in a straight fashion, while further peaks at integer multiples of this ΔI correspond to molecules passing through in differing folded states (2 or more double-helical strands of the DNA occupying the pore at a time).[25] From analysis of the translocation event rates (see Supporting Information, Figure S3), we have determined that the probability of two molecules traversing the pore simultaneously is extremely low, even at the highest applied voltages applied in our experiments; thus the peaks in the histograms correspond to single molecules translocating the nanopore. The red dotted lines spaced along the y-axis of the translocation traces (Figure 2) correspond to integer multiples of the fitted values of ΔI, and these correspond well to the levels of current observed within each trace, as expected.

When RNA molecules are translocated through our nanopores at low voltage, a similar behavior is observed. In the case of ds A-RNA, translocation events can be identified as before, and the current histogram reveals multiple distinct peaks, as in the case of dsDNA (Figure 2b, histogram of data at 100 mV). As the subsequent current blockades are again integer multiples of each other, these events likely correspond to molecules traversing the pore in different folded states. Similarly, histograms were made from the events detected when single-stranded homopolymers were translocated at low bias, showing again a clearly distinguishable peak relative to the baseline (see Supporting Information, Figure S4).

We next repeated these measurements at higher voltages to determine the effect of voltage on molecule translocation. In practice, we found that effects such as pore instability and clogging limited the practically achievable maximum voltage to 600 mV. When the measurements were repeated

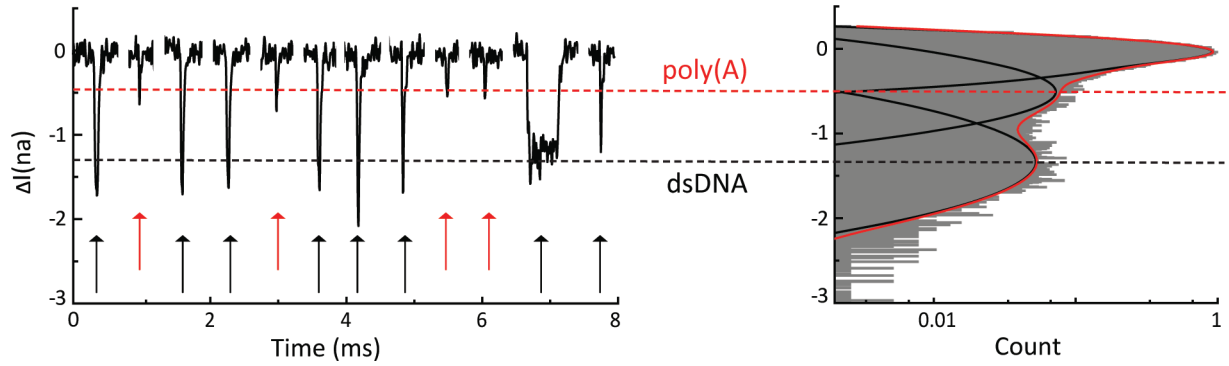

Figure 4. Experiment to test ability to discriminate double- and single-stranded nucleic acids. Translocation experiment, with equimolar concentrations of 12.7 kb DNA and poly(A). Data was taken at 600 mV in a 10 nm nanopore and was digitally filtered at 35 kHz. A sample of events is shown on the left, and the resulting current blockade histogram is seen on the right. Two well-separated peaks of ΔI are seen, each corresponding to either dsDNA or poly(A). Relating these peak values to the events themselves, it then becomes possible to individually identify the molecule involved from only a single translocation event, as indicated by the red and black arrows.

at these higher applied biases, events could still be detected, albeit with shorter translocation times, and the current histograms predominantly revealed a single peak for all molecules studied (Figure 2a−e, right panels). We constructed such histograms for each molecule tested throughout the entire voltage range of 100 to 600 mV at 50 mV increments, and we repeated these measurements in several nanopores. We then looked at the voltage dependence of the conductance change, $\Delta G = \Delta I/V$, for the first peak in each histogram for each molecule studied (Figure 3a). ΔG was selected as the parameter of interest, as it allows normalized comparison of blockades between different experiments on pores of similar size. The translocation times are not discussed in great detail here because of the large variation in length of the RNA molecules. In all cases, the translocation time decreased as the voltage was increased, as expected (Supporting Information, Figure S5). In certain cases, the translocation times were unexpectedly long, which might be attributed to interactions with the nanopore walls, but these did not affect the conductance blockade. No relationship between ΔG and the translocation times was observed.

Double-Stranded Nucleic Acids Exhibit an Increasing Current Blockade at Increasing Bias Voltage. We will first discuss the response of ΔG to voltage for the double-stranded nucleic acids. In the case of dsDNA (Figure 3a, black circles), we observe that the current blockade increases as the applied bias voltage increases from 100 to 600 mV. The measured values for ΔG at 600 mV is dsDNA = 2.25 ± 0.09 nS (versus ∼1.6 ± 0.5 nS at 100 mV). The errors in our values of ΔG reflect the maximum and minimum values from multiple experiments (see Figure 3a caption, and Supporting Information Figure S6 showing all individual measurement points). The ΔG for the ds A-RNA also increases with increasing bias, but the effect is somewhat less pronounced than for ds B-DNA (Figure 3a, blue circles). These results suggest that the molecules are actually occupying a larger effective volume in or close to the nanopore at higher voltage, increasingly contributing to the pore resistance as the applied bias increases. Possible explanations for this unexpected result are discussed below.

Single-Stranded Homopolymers Exhibit a Decreasing Current Blockade at Increasing Applied Bias Voltage. In contrast to the behavior observed for the double-stranded polymers, as the applied voltage was increased, the values for ΔG showed a very pronounced decrease for the single-stranded RNA homopolymers poly(A), poly(C), and poly(U) (Figure 3a, red, violet, and green circles, respectively). At low applied bias voltage (100 mV), the ΔG values for all three homopolymers were indistinguishable, both from each other and from the double-stranded molecules (all yielding ∼1.6 nS). But as the voltage increases up to 600 mV, the ΔG were reduced to 0.95 ± 0.04 nS (poly(A)), 0.65 ± 0.11 nS (poly(C)), and 0.58 nS (poly(U)). Interestingly, at these higher applied bias limits, the purine poly(A) and the pyrimidines poly(U) and poly(C) can also be well separated (Figure 3a).

Individual Double and Single-Stranded Translocation Events Can Be Distinguished at High Applied Bias Voltage. We have carried out a mixing experiment to see whether the application of high voltages allows for rapid discrimination between single- and double-stranded nucleic acids, using the large difference in conductance change between double- and single-stranded molecules. High voltages should also facilitate such separation, as in this regime all current histograms consist of only single peaks. As a proof-of-principle, approximately equimolar amounts of 12.7 kb DNA and poly(A) molecules were mixed and translocated through the nanopore as before. A series of events from this mixing experiment are shown at left in Figure 4, displaying differing values of the current blockade. The histogram of these blockade currents demonstrates two well-separated peaks, presumably corresponding to the translocation of either poly(A) or dsDNA, respectively (Figure 4). Values for ΔG for each molecule determined from this mixing experiment were dsDNA = 2.23 nS and poly(A) = 0.81 nS. This difference in the conductance change is consistent with the values measured for each molecule in isolation, and it is clear that the two different molecule populations can be distinguished. On the basis of the average ΔG computed, the suggested attribution of individual events to the translocation

of dsDNA versus poly(A) molecules is indicated in Figure 4 by black and red arrows, respectively.

Discussion. We have successfully translocated both double-stranded as well as various types of single-stranded RNA molecules through solid-state nanopores. The homopolymeric nature of the single-stranded RNA molecules eliminated any potential contributions of internal basepairing to the signal of the molecules traversing the nanopore, under normal conditions without the need for denaturarants. As the homopolymers do have a widely dispersed length, we have focused on the magnitude of the conductance blockade rather than the pore dwell times, as the latter information is obscured by the molecular length variations. As shown, translocation of single- versus double-stranded molecules across a wide range of applied bias voltages yields surprisingly different molecular signatures.

In the case of the double-stranded molecules, we observe a slightly increasing ΔG as a function of the applied bias voltage. If the molecules occupied the same fraction of pore volume at every applied bias, we would expect ΔG to remain constant, based on a geometrical argument relating ΔG to the amount of ions excluded by the molecule passing through the pore.[34] Since the persistence length L_p for dsDNA and dsRNA are ~50 and ~60 nm, respectively, these molecules are expected to be fully taut inside the nanopore. Therefore, any further changes in the measured ΔG must be due to either some form of distortion of the molecular structure within the pore or changes in access resistance due to the presence of the DNA residing just outside the pore. A similar effect has been observed for long molecules of DNA in small pores (3−8 nm),[36] where it was argued that the access resistance is increased for longer molecules due to their larger radius of gyration and subsequent enhanced interactions of the DNA with the pore membrane. It is possible that these DNA-membrane interactions are further enhanced at higher voltages, thus explaining the increased conductance blockade that we measure. As the applied bias is increased and the molecule is pulled more strongly toward the pore, perhaps it is driven to a greater level of interaction with the pore membrane. A similar argument would apply for the dsRNA, but not for the homopolymers, as these molecules have much smaller radii of gyration ($R_{g,poly(A)} \sim 50-100$ nm, $R_{g,DNA} \sim$ 500 nm) and this effect would therefore be much less pronounced.

The ss homopolymers display a very different dependence of the ΔG on voltage, namely a monotonic decrease, and we now discuss possible explanations for this. It is known that poly(A)[22] and poly(C)[37] both adopt a helical conformation in solution (Figure 1d). Since these helices can be unwound at moderate forces of the order 10−30 pN,[38] it is possible that the decrease in ΔG that we observe for the homopolymers is at least partly due to such force-induced denaturation of the base-stacking in these molecules. However, we observed the same decrease in ΔG for poly(U) (Figure 3a), which is known to adopt a random-coil structure in solution at room temperature.[24,39] On this basis, we consider it unlikely that such a helix−coil transition would provide the dominant contribution to the observed decrease in ΔG with voltage.

An alternative explanation for this decreasing ΔG relies on the different degrees of flexibility between single- and double-stranded molecules. Since the single-stranded homopolymers are much more flexible than the double-stranded molecules (homopolymer $L_p \sim 1$ nm, dsDNA $L_p \sim 50$ nm),[38,39] these molecules will be significantly coiled by the entropic forces on the length scale of the nanopore. We therefore considered that the observed decreasing ΔG values might be due to stretching of these molecules inside the pore resulting from the electric field and opposing drag forces (Figure 3b); at higher voltages V, the average stretching force F also increases. On the basis of this argument, at low forces (Figure 3c) the molecule has a lower relative extension, $x/L_0 < 1$ (with L_0 the contour length of the molecule); thus, more polymer material would occupy the volume within the nanopore, resulting in a higher ΔG value. At higher forces (Figure 3d), the molecule will be stretched out more within the nanopore, and the total volume blocking the nanopore will be correspondingly reduced, resulting in a lower ΔG. This argument does not apply to the double-stranded molecules, as their much larger persistence length ensures that such entropic coiling within the pore is negligible.

To test whether this effect could account for the experimental observations, we have fitted the ΔG values for the homopolymers with a simple model based on the well-accepted wormlike chain description of polymer stretching[40] (Figure 3a, solid lines). The wormlike chain model relates the stretching force F on a polymer to its fractional extension, x/L_0. Our model assumes that the conductance change ΔG is inversely related to the relative extension x/L_0, such that low x/L_0 results in high ΔG, and vice versa; $\Delta G = (b)/(c + x/L_0)$, where b and c are fit parameters. Next, we assume that the stretching force F is proportional to the applied bias voltage,[18] $F = \sigma \cdot V$, where σ is a conversion constant in pN/mV. Making these substitutions into the wormlike chain model (Supporting Information) results in a relationship between the applied voltage and ΔG

$$V(\Delta G) = a\left\{\frac{1}{4\left(1 - \frac{b}{\Delta G} + c\right)^2} - \frac{1}{4} + \frac{b}{\Delta G} - c\right\} \tag{1.1}$$

where a, b, and c are free-fitting parameters. The red, violet, and green solid lines in Figure 3a are fits of this model to our data and can be seen to describe trends observed in the data well. Note that the wormlike chain description assumes that a constant force acts on the polymer ends, which may not be strictly true in our case. The stretching force arises from a complicated combination of electrical forces and viscous drag forces and is expected to vary in magnitude along the polymer, peaking at some point above the nanopore (Figure 3d) where the molecule may not yet sense the influence of the electrical field. For simplicity, however, we have assumed that the integral of this stretching force over the entire region of the nanopore simply leads to an average extension x/L_0 of the molecule inside the pore.

From the resulting fit parameters, we can extract values for the conductance blockade ΔG_{max} at zero extension ($x/L_0 = 0$), ΔG_{min} at full extension ($x/L_0 = 1$), and the conversion constant σ relating the applied voltage to an effective stretching force. The values we find for ΔG_{max} are 1.86 ± 0.48 nS for poly(A), 5.53 ± 4.25 nS for poly(C), and 4.22 ± 1.77 nS for poly(U). In this case, the polymer experiences no force and can be approximated as a random coil of approximate volume $V = (4/3)\pi R_g^3$ (with where R_g is the radius of gyration). One can estimate that the relative volume comprised by the polymer itself is on the order of 1−5% for the homopolymers used here (using different persistence lengths for the homopolymers from Seol, et al.[38,39]). Thus, approximately 1−5% of the pore volume (and thus of the ionic current) will be blocked by the polymer. Given that the total conductance for a 10 nm nanopore is about 75−80 nS, the values of ΔG_{max} are in good agreement with this, assuming that the conductance blockade is indeed proportional to the volume occupied by the polymer inside the nanopore.

Second, we can compare the plateau values ΔG_{min} derived from our fit to the expected blockade for single-stranded molecules passing through the pore in a fully stretched manner, based on simple volumetric comparison of the molecules. Again, if the conductance blockade is indeed proportional to the volumes occupied by these molecules inside the nanopore, the ΔG_{min} values from our fit would reflect the volume occupied by the fully stretched homopolymers. We therefore determined the solvent inaccessible volumes of equally long sections of the fully stretched homopolymers and compared these to that of DNA from our computer models (Methods). We find the following volume ratios $V_{poly(A)}/V_{DNA} = 0.34$, $V_{poly(C)}/V_{DNA} = 0.26$, and $V_{poly(U)}/V_{DNA} = 0.31$. These are to be compared to the ratios $\Delta G_{min}/\Delta G_{dsDNA}$ that we deduce from the fits, where ΔG_{dsDNA} (= 1.6 ± 0.5 nS) equals the value of ΔG at 100 mV, selected as the ΔG for DNA at higher voltages of 600 mV is unexpectedly high. These ratios equal 0.41 ± 0.12 for poly(A), 0.25 ± 0.18 for poly(C), and 0.18 ± 0.13 for poly(U), which is in reasonable agreement with the expected values. However, we note that van Dorp et al. have observed that even in the static situation where DNA is arrested in the nanopore using optical tweezers, a full explanation of ΔG is challenging[41] due to the unknown effects of the molecule above the nanopore on the access resistance of the nanopore. More precise agreement would require further investigation of this issue.

Finally, we can extract the value of σ from the fit. Optical tweezer measurements on stalled dsDNA inside a nanopore yielded a force of ~24 pN/100 mV or $\sigma = 0.24$ pN/mV in pores of similar size as used in this study. Taking into account the approximately 2−3-fold lower charge density for a single-stranded homopolymer at almost full extension, we would expect $\sigma \sim 0.1$ pN/mV in our case. However, the value for σ that we find from our fit is significantly lower, $\sim 0.008 \pm 0.004$ pN/mV. Potential reasons for this discrepancy include the fact that in our experiments the molecules are moving, which may yield quite different forces acting on the polymer. It is also possible that the charge screening and subsequent drag forces of the counterions may be significantly different for single-stranded polymers than for DNA, which might give rise to a lower force. Future experiments with optical tweezers probing the stretching force on the homopolymers could shed light on these issues.

An exciting prospect is that the distinctive ΔG values observed for each molecule at high applied bias imply that one could use solid-state nanopores to discriminate between single and double-stranded nucleic acid molecules based on current blockade; and it may even be possible to use this phenomenon for discriminating purine and pyramidine bases (Figure 3a). In our proof-of-principle "mixing" experiment (Figure 4) at a voltage of 600 mV, dsDNA exhibits a larger current blockade than poly(A) molecules at the same voltage. Potentially, by counting the numbers of translocation events of each kind, it could become possible to measure the absolute concentrations of each of double and single-stranded nucleic acid molecules within a mixture in a single measurement. This type of application amounts to molecular "Coulter Counting"[42] and could have wide utility in measuring absolute concentrations of diverse biopolymer mixtures in a single measurement.

Acknowledgment. We thank S. W. Kowalczyk, A. R. Hall, M. Y. Wu, and V. Svechnikov for fabrication of the nanopores, S. Hage, S. Donkers for assistance with molecule preparation, and J. van der Does and J. Beekman for assistance with instrument construction. We especially thank I. Vilfan for his expertise in handling and the preparation of our RNA molecules. We also wish to thank S. Lemay and K. Visscher for their valuable discussions. N. H. D. acknowledges financial support from the TU Delft, from the Netherlands Organisation for Scientific Research (NWO) via a Vidi grant, and from the European Science Foundation via an EURYI award.

Note Added after ASAP Publication: This paper was published ASAP on July 19, 2009. The Acknowledgment was updated. The revised paper was reposted on July 23, 2009.

Supporting Information Available: This material is available free of charge via the Internet at http://pubs.acs.org.

References

(1) Bustamante, C.; Bryant, Z.; Smith, S. B. 2003, *421*, (6921), 423−427.
(2) Larson, M. H.; Greenleaf, W. J.; Landick, R.; Block, S. M. *Cell* **2008**, *132* (6), 971–982.
(3) Liphardt, J.; Onoa, B.; Smith, S. B.; Tinoco, I. J.; Bustamante, C. *Science* **2001**, *292* (5517), 733–7.
(4) Onoa, B.; Dumont, S.; Liphardt, J.; Smith, S. B.; Tinoco, I., Jr.; Bustamante, C. *Science* **2003**, *299* (5614), 1892–1895.
(5) Dekker, C. *Nat Nanotechnol.* **2007**, *2* (4), 209–15.
(6) Healy, K.; Schiedt, B.; Morrison, A. P. *Nanomedicine* **2007**, *2* (6), 875–897.
(7) Deamer, D. W.; Akeson, M. *Trends Biotechnol.* **2000**, *18* (4), 147–151.
(8) Kasianowicz, J. J.; Brandin, E.; Branton, D.; Deamer, D. W. *Proc. Natl. Acad. Sci. U.S.A.* **1996**, *93* (24), 13770–13773.
(9) Smeets, R. M.; Kowalczyk, S. W.; Hall, A. R.; Dekker, N. H.; Dekker, C. *Nano Lett.* [Online] **2008**, DOI: 10.1021/nl803189k (accessed December 3, 2008).

(10) Song, L.; Hobaugh, M. R.; Shustak, C.; Cheley, S.; Bayley, H.; Gouaux, J. E. *Science* **1996**, *274* (5294), 1859–1865.
(11) Kang, X.-f.; Cheley, S.; Rice-Ficht, A. C.; Bayley, H. *J. Am. Chem. Soc.* **2007**, *129* (15), 4701–4705.
(12) Meller, A.; Nivon, L.; Branton, D. *Phys. Rev. Lett.* **2001**, *86* (15), 3435.
(13) Khulbe, P. K.; Mansuripur, M.; Gruener, R. *J. Appl. Phys.* **2005**, *97* (10), 104317.
(14) Mathe, J.; Visram, H.; Viasnoff, V.; Rabin, Y.; Meller, A. *Biophys. J.* **2004**, *87* (5), 3205–12.
(15) Akeson, M.; Branton, D.; Kasianowicz, J. J.; Brandin, E.; Deamer, D. W. *Biophys. J.* **1999**, *77* (6), 3227–3233.
(16) Li, J.; Gershow, M.; Stein, D.; Brandin, E.; Golovchenko, J. A. *Nat. Mater.* **2003**, *2* (9), 611–615.
(17) Storm, A. J.; Chen, J. H.; Ling, X. S.; Zandbergen, H. W.; Dekker, C. *Nat. Mater.* **2003**, *2* (8), 537–40.
(18) Keyser, U. F.; Koeleman, B. N.; van Dorp, S.; Krapf, D.; Smeets, R. M. M.; Lemay, S. G.; Dekker, N. H.; Dekker, C. *Nat. Phys.* **2006**, *2* (7), 473–477.
(19) Storm, A. J.; Storm, C.; Chen, J.; Zandbergen, H.; Joanny, J.-F.; Dekker, C. *Nano Lett.* **2005**, *5* (7), 1193–1197.
(20) Trepagnier, E. H.; Radenovic, A.; Sivak, D.; Geissler, P.; Liphardt, J. *Nano Lett.* **2007**, *7* (9), 2824–2830.
(21) McNally, B.; Wanunu, M.; Meller, A. *Nano Lett.* **2008**, *8* (10), 3418–3422.
(22) Saenger, W.; Riecke, J.; Suck, D. *J. Mol. Biol.* **1975**, *93* (4), 529–534.
(23) Arnott, S.; Chandrasekaran, R.; Leslie, A. G. *J. Mol. Biol.* **1976**, *106* (3), 735–48.
(24) Saenger, W. *Principles of Nucleic Acid Structure*. Springer-Verlag: New York, 1984; p 556.
(25) Storm, A. J.; Chen, J. H.; Zandbergen, H. W.; Dekker, C. *Phys. Rev. E* **2005**, *71* (5), 051903.
(26) Gershow, M.; Golovchenko, J. A. *Nat. Nanotechnol.* **2007**, *2* (12), 775–9.
(27) Vilfan, I. D.; Candelli, A.; Hage, S.; Aalto, A. P.; Poranen, M. M.; Bamford, D. H.; Dekker, N. H. *Nucleic Acids Res.* **2008**, *36* (22), 7059–67.
(28) van den Hout, M.; Hage, S.; Dekker, C.; Dekker, N. H. *Nucleic Acids Res.* **2008**, *36* (16), e104.
(29) Broido, M. S.; Kearns, D. R. *J. Am. Chem. Soc.* **1982**, *104* (19), 5207–5216.
(30) Shenogin, S.; Ozisik, R. *Polymer* **2005**, *46* (12), 4397–4404.
(31) Drew, H. R.; Samson, S.; Dickerson, R. E. *Proc. Natl. Acad. Sci. U.S.A.* **1982**, *79* (13), 4040–4044.
(32) Liu, L.; Botos, I.; Wang, Y.; Leonard, J. N.; Shiloach, J.; Segal, D. M.; Davies, D. R. *Science* **2008**, *320* (5874), 379–381.
(33) Storm, A. J.; Chen, J. H.; Zandbergen, H. W.; Dekker, C. *Phys. Rev. E: Stat., Nonlinear, Soft Matter Phys.* **2005**, *71* (5 Pt 1), 051903.
(34) Smeets, R. M. M.; Keyser, U. F.; Krapf, D.; Wu, M.-Y.; Dekker, N. H.; Dekker, C. *Nano Lett.* **2006**, *6* (1), 89–95.
(35) Fologea, D.; Gershow, M.; Ledden, B.; McNabb, D. S.; Golovchenko, J. A.; Li, J. *Nano Lett.* **2005**, *5* (10), 1905–1909.
(36) Wanunu, M.; Sutin, J.; McNally, B.; Chow, A.; Meller, A. *Biophys. J.* **2008**, *95* (10), 4716–4725.
(37) Arnott, S.; Chandrasekaran, R.; Leslie, A. G. W. *J. Mol. Biol.* **1976**, *106* (3), 735–748.
(38) Seol, Y.; Skinner, G. M.; Visscher, K.; Buhot, A.; Halperin, A. *Phys. Rev. Lett.* **2007**, *98* (15), 158103.1158103.4.
(39) Seol, Y.; Skinner, G. M.; Visscher, K. *Phys. Rev. Lett.* **2004**, *93* (11), 118102.1118101.4.
(40) Marko, J. F.; Siggia, E. D. *Macromolecules* **1995**, *28*, 8759–8770.
(41) van Dorp, S.; Keyser, U. F.; Dekker, N. H.; Dekker, C.; Lemay, S. G. *Nat. Phys.* [Online early access], DOI: 10.1038/nphys1230 (accessed March 29, 2009).
(42) Coulter, W. H. U.S. Patent No. 2,656,508, Oct 20. 1953.
(43) Tabard-Cossa, V.; Trivedi, D.; Wiggin, M.; Jetha, N. N.; Marziali, A. *Nanotechnology* **2007**, *18*, 05505.

NL901370W